Minimisation of Pressure Loss by Optimising the CO Removal Stage in PEM Fuel Cell Heating Appliances

Main author
Markus Wolf
Karlsruhe Institute of Technology (KIT), Engler-Bunte Institut,
Division of Fuel Chemistry and Technology, Karlsruhe, Germany

Co-authors
Gregor Worringer
Rainer Reimert

1. Abstract

Reducing the pressure-loss of a stationary natural gas fed fuel cell below the grid pressure avoids the need of a process gas compressor, thus auxiliary power consumption would be lowered and overall system efficiency increased. This and a simplification in design will improve the economics of PEM fuel cell systems and will promote their commercialisation. This goal can be achieved through optimisation of the CO-removal section within the fuel processor by reducing the number of required process steps using catalysts of high activity supported by metallic monoliths and by optimisation of the fuel processor's temperature profile.

2. Minimisation of Pressure Loss by Optimising the CO Removal Stage in PEM Fuel Cell Heating Appliances

2.1 Motivation

To supply a hydrogen-rich fuel gas to a PEM fuel cell heating appliance, natural gas is processed in several series-connected reactors, and the processed gas passes heat exchangers, bends and a mixer. Each part of this chain is accompanied by a loss in pressure. Therefore, the low gauge pressure of distribution networks challenges the design of PEM fuel cell heating appliances.

The PEM fuel cell itself requires approximately half of the pressure of 20 mbar above ambient available in a distribution network /1/ for its operations /2/. Only approx. 10 mbar of pressure is therefore left for fuel gas processing. Compressing the gas upstream of the fuel cell system or within it is no favourable option in terms of energy because of the low compressor efficiencies at the relevant output range. A more economical approach to the pressure situation in the appliances is therefore desirable. An important process step in fuel gas treatment is catalytic CO conversion. The conversion usually comprises a preliminary and a final stage with up to three reactors and three heat exchangers in the most unfavourable design (Fig. 5).

The paper aims at identifying measures to minimise the pressure loss in stationary PEM fuel cell heating appliances operated on natural gas. Reduced pressure loss and a less complex design will help to improve the economics as well as the competitive position of PEM fuel cell heating appliances for use in residential heat and power generation. The work focuses on the use of metal honeycomb reactors and on the reduction of the number of CO removal stages for the product gas that is obtained from natural gas reforming.

2.2 Water gas shift catalysts

The water gas shift reaction (WGS) is a typical heterogeneous reaction of gas phase reactants on a solid phase catalyst. The reaction which is slightly exothermic, converts the CO to CO_2 and H_2 according to Eq. (1).

$$CO + H_2O \rightleftharpoons CO_2 + H_2 \qquad \Delta_R H_{25°C} = -41{,}1\ \text{kJ/mol} \qquad (1)$$

Due to its exothermic nature, at low temperature the forward reaction to H_2 and CO_2 is favoured while at high temperature the reverse reaction dominates. In current commercial application the WGS reaction is carried out in two stages, a high temperature shift (HTS) and a low temperature shift (LTS), which utilize different catalysts. The HTS catalysts operate at a temperature range of 320 – 500 °C, whereas the LTS catalysts operate at 200 – 270 °C (Fig. 1).

Commercially available are the iron-based HTS-, the copper-based LTS-catalyst, and in between the platinum-based MTS-catalyst. All the three catalysts purposely exhibit only a small range of operating temperature (Fig. 2). The iron- and the platinum based catalysts catalyse also the methanation reaction and consequently consume a part of the formed hydrogen /3/.

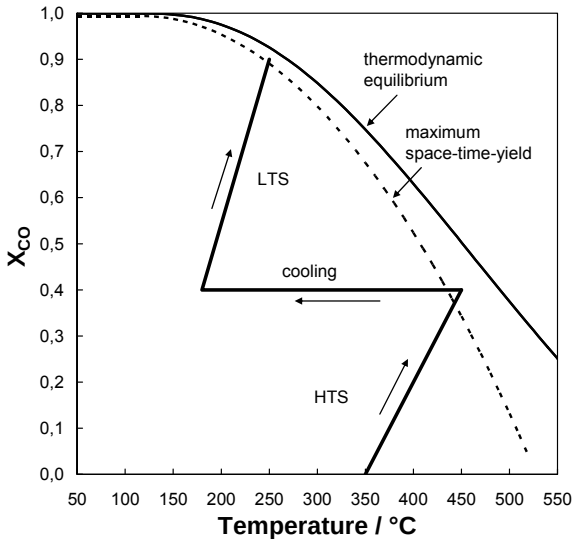

Fig. 1: Commercially realized and ideal (maximum space-time-yield) temperature profiles for the CO-conversion by WGS.

Grenoble et al /3/ studied in detail the WGS over supported noble metals at atmospheric pressure and in the temperature range of 270 – 380 °C. alumina-supported noble metals exhibited higher activity than catalysts carried on silica or on activated carbon. Though gold was considered an essentially inactive metal for catalysis until the 1980s, academic research revealed that very fine gold particles supported on Fe_2O_3 and TiO_2 exhibiting an intimate contact between the gold particles and the support show reasonable catalytic activity, e.g. for the oxidation of CO at low temperature but also for the WGS /5/. Hence, gold seems to be a promising alternative to platinum catalysts in fuel cell driven applications /6/. However, platinum is the only commercially applied noble metal based WGS catalysts.

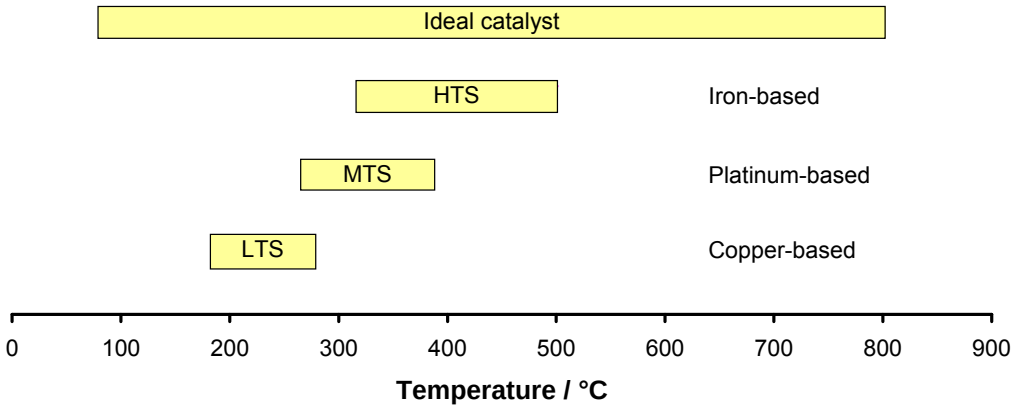

Fig. 2: Comparison of the working temperature ranges of an ideal catalyst and the commercially available /4/.

2.2 Selection of catalyst

Metal honeycombs were impregnated with the preselected catalytic systems Au/CeO_2, Pt/CeO_2, Ru and Cu/ZnO and examined for their CO conversion behaviour under the operating conditions of a fuel cell heating system.

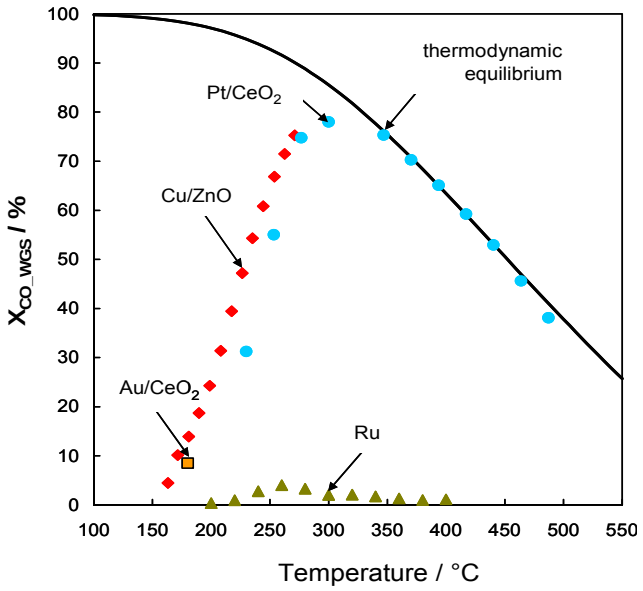

Fig. 3: Comparison of WGS catalysts' activities regarding WGS reaction, GHSV = $V_{converter}/ {}^{N}\Phi_{gas}$ = 650 h^{-1}, inlet gas composition 9.24 % CO, 0.48 % CH_4, 7.36 % H_2, 27,36 % H_2O, (all percentages per volume) atmospheric pressure /7/.

It was found that the Cu/ZnO catalyst had the highest CO conversion activity accompanied by a very high selectivity level with respect to the water gas shift reaction (WGS) (Fig. 3).

Activation of the Cu/ZnO catalyst required prior to its use is a disadvantage. However, pre-reduced and stabilised $Cu/ZnO/Al_2O_3$ catalysts are available for industrial applications; their application could eliminate the need for pre-treatment of the catalyst in place /6/. Pyrophoric behaviour of the hot catalyst when in contact with atmospheric oxygen is to be expected during start-up and shut-down of the PEM fuel cell heating system. As a counter-measure the system could, for example, be rendered inert with non-reformed natural gas. Pt/CeO_2 might be a promising alternative to $Cu/ZnO/Al_2O_3$.

2.4 Potential of metal honeycombs

The pressure loss for honeycomb reactors is usually one to two orders of magnitude lower than for conventional catalyst beds for the same height of bed (and for the same surface-to-volume ratio) /7/.

Also, metal honeycombs have reasonably high heat conductivity. Thanks to the catalyst support geometry, the reaction heat released in the catalyst layer is removed promptly and effectively through the honeycomb material. This superior performance can probably be enhanced further by optimising passage diameters and by use of metals with higher heat conductivities. Simply replacing the existing honeycomb material by copper will increase the effective heat conductivity by two to three orders of magnitude.

The geometry of the honeycombs also favoures temperature control. Several configurations for heat transfer are possible; for example, cooling via an outer shell and/or inclusion of cooling canals in the honeycomb structure itself /7/ (Fig.4).

Fig. 4: Heat transfer configurations for metallic honeycomb structures /7/.

Both configurations are similar to tube and shell heat exchangers or reactors. Another possibility would be to provide intermediate cooling between two honeycombs in series, similar to a staged reactor.

When using metal honeycombs, a narrow distribution of the honeycomb passage diameters is essential as the gas residence times should be as similar as best possible in all passages to achieve high conversion rates.

2.5 Reaction control

The way heat is removed from or kept within the reactors determines the temperature profiles along the CO-conversion path. In order to optimize the temperature over the process the WGS and the methanation reactors were coupled in a mathematical model. Applying the formerly experimentally acquired reaction kinetics the complete CO-conversion scheme was simulated. The need for heat exchangers between the reactors was eliminated by maintaining the temperature at the WGS reactor outlet and the temperature at the methanation reactor inlet on the same level. While maintaining identical inlet conditions, the simulations allowed comparing reactor lengths and product gas compositions at different temperature levels.

For calculating the WGS reaction kinetic data, obtained by measurements with a pulverized $Cu/ZnO/Al_2O_3$ catalyst in a fixed bed reactor, were used (Tab. 2). The reactor inlet temperature was set below 300 °C due to thermal stability of the catalyst. The lower limit of the exit temperature depends on the activity of the WGS catalyst, but should be in the operating range of the ruthenium catalyst, so WGS could be coupled properly with the methanation reactor. Below 190 °C the activity of the WGS catalyst was found to be unsatisfactory.

For calculating the CO-methanation rates of a Ru catalyst the equations (4), (5) and (6) in table 1 were used. They were extracted from /6/ with some variation. The formal equation system was derived from a methanation reaction at similar conditions but at 4 bars. It describes the formation of methane through hydrogenation of CO and CO_2, and the formation of long-chain hydrocarbons. For the application of the equation system at 1 bar it was assumed that the latter reactions are negligible at the low pressure applied here. This assumption was confirmed by measurements at 1 bar.

$$r_{i,j} = \frac{dp_i}{d\tau_{\mathrm{mod}}} \qquad i\text{: reactand, } j\text{: reaction} \qquad (2)$$

Tab.1: Used kinetic expressions for dimensioning WGS /7, 8/ and methanation /9/ reactors. $r_{i,j}$: reaction rate, k frequency factor, K: equilibrium coefficient, E_A: activity energy and $\Delta_S H$: adsorption energy.

WGS	**Methanation**
$r_{WGS,CO} = k \cdot p_{CO} \cdot p_{H_2O} \cdot (1-\beta)$ (2)	$r_{Meth,CO} = -R \cdot T \left(\frac{k_1 \cdot K_C \cdot K_H^2 \cdot p_{CO}^{0.5} \cdot p_{H_2}}{\left(1 + K_C \cdot p_{CO}^{0.5} + K_H \cdot p_{H_2}^{0.5}\right)^3} + \frac{k_3 \cdot K_C^2 \cdot p_{CO}}{\left(1 + K_C \cdot p_{CO}^{0.5} + K_H \cdot p_{H_2}^{0.5}\right)^2} \right)$ (4)
$\beta = \frac{p_{CO_2} \cdot p_{H_2}}{p_{CO} \cdot p_{H_2O} \cdot K_p(T)}$ (3)	$r_{Meth,CO_2} = -R \cdot T \frac{k_2 \cdot p_{CO_2}^{0.14}}{\left(1 + K_C \cdot p_{CO}^{0.5}\right)^2}$ (5)
	$r_{Meth,CH_4} = R \cdot T \left(\frac{k_1 \cdot K_C \cdot K_H^2 \cdot p_{CO}^{0.5} \cdot p_{H_2}}{\left(1 + K_C \cdot p_{CO}^{0.5} + K_H \cdot p_{H_2}^{0.5}\right)^3} + \frac{k_2 \cdot p_{CO_2}^{0.14}}{\left(1 + K_C \cdot p_{CO}^{0.5}\right)^2} \right)$ (6)
Arrhenius parameters: $k_0 = 5.811 \cdot 10^{-8}$ mol/(g·s·Pa²) $E_A = 57.63$ kJ/mol	Arrhenius parameters: $k_{0,1} = 5.7 \cdot 10^{7}$ mol/(g·s) $E_{A,1} = 97.4$ kJ/mol $k_{0,2} = 1.3 \cdot 10^{8}$ mol/(g·s·bar^{0,14}) $E_{A,2} = 123$ kJ/mol $K_C = 5.5 \cdot 10^{-6}$ bar$^{-0,5}$ $\Delta_S H_C = -63.5$ kJ/mol $K_H = 1{,}6 \cdot 10^{-4}$ bar$^{-0,5}$ $\Delta_S H_H = -36.2$ kJ/mol

To calculate the length of the metallic monolith reactor, some assumptions were made:

- The monolith presumably is a bundle of cylindrical channels with equal diameters of 1 mm.
- All the channels have the same pressure loss, mass flow, catalyst loading and constant radial temperature, thus equation (7) can be applied.

This simplification allows for the scale up from one channel to the total monolith.

Furthermore for the gas flow in the channels the characteristics of an ideal plug flow reactor were assumed. The reactions were considered as quasi-homogeneous gas phase reactions. The eligibility of this simplification was proven by the CFD simulation of one reactor channel with heterogeneous reaction on the catalyst surface. In comparison to a homogeneous gas phase reaction simulation the results showed a negligible discrepancy. Isothermal, adiabatic and ideal (Fig. 1) temperature profiles were calculated for the WGS whereas adiabatic conditions were considered for the methanation reaction. The model parameters are listed in Tab.2:

Tab.2: Parameters used for modelling the CO-converter.

Channel diameter in mm	1
Velocity in m/s	0.5 (at 200 °C)
Pressure	1 bar
catalyst loading in kg/m³	500

$$\tau_{\mathrm{mod}} = \frac{m_{Kat}}{\Phi^{V}} = c_{CO,0} \cdot \int_{0}^{U_{CO,outlet}} \frac{dU_{CO}}{-r_{CO}} \qquad (7)$$

The simulation results indicate firstly that WGS can be performed in one step. Secondly, both the WGS and the methanation should be operated in an isothermal mode in a temperature range from 240 °C to 260 °C considering the intended catalyst operating range and achievable hydrogen concentration of approximately 80 % in the dry product gas. At 260 °C, the required reactor volume is less than 70 % of that at 240 °C, respectively. But it needs to be examined in this context how the higher temperature affects catalyst life. The reactors currently used in fuel cell systems are operated at 240 °C /2/. In the proposed operating range the total pressure loss is less than 4 mbar for the entire CO conversion stage.

3. Conclusion

Because of their relatively low pressure loss in the intended application, metal honeycomb reactors are a reasonable alternative to conventional catalyst beds. Compression of the process gas would no longer be necessary. This reduces parasitic energy consumption and improves total efficiency of the PEM fuel cell heating system.

When using metal honeycomb reactors coated with Cu/ZnO/Al_2O_3 as catalyst for the WGS reaction, a high-temperature shift stage is no longer necessary, thus eliminating the need for one reactor and one heat exchanger in the design. The WGS reactor outlet temperature is in the operating window of the methanation catalyst used for final CO-conversion, thus eliminating the need for another heat exchanger. Fig. 5 compares the simplified design with the initial.

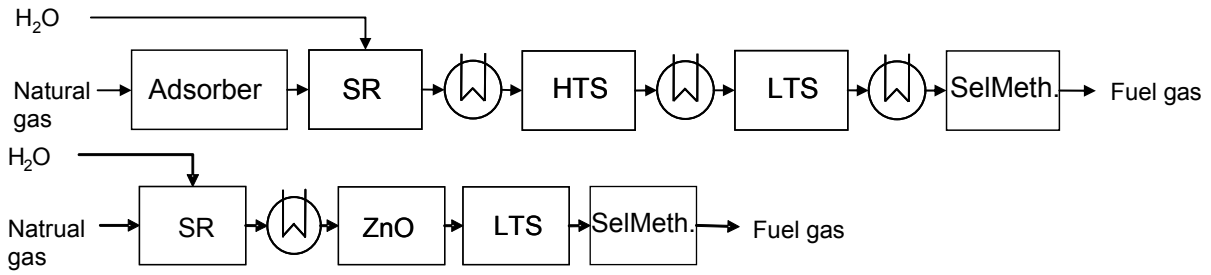

Fig. 5: Simplified fuel gas supply to PEM fuel cell heating appliance. Top: initial design. Bottom: simplified design. SR: steam reforming. HTS: high-temperature shift reaction. LTS: low-temperature shift reaction. SelMeth: selective methanation.

References

/1/ Technical Rules: DVGW Code of Practice G 260, Bonn, May 2008.

/2/ Britz, P., Zartenar, N.:
PEM - Fuel Cell Systems for Residential Applications
Fuel Cells, 4 (2004), 4, 269-275.

/3/ Grenoble, D.C.; Estadt, M.M.; Ollis, D.F.:
The Chemistry and Catalysis of the Water Gas Shift Reaction
J. Catal., 67 (1981), 90-102

/4/ Wolf, M.; Worringer, G.; Reimert, R.:
Optimisation of the CO-Converter for a PEM Fuel Cell
In: Proceedings of the 2008 International Gas Research Conference,
October 8-10, Paris, France

/5/ Haruta, M.:
Catalysis of Gold Nanoparticles Deposited on Metal Oxides
Cattech, 6 (2002), Nr. 3, 102-115

/6/ Hinrichsen, K.-O.; Kochloefl, K.; Muhler, M.:
Volume 6, Chapter 13.12, Water Gas Shift and COS Removal
Handbook of Heterogeneous Catalysis
2nd Edition, Weinheim, Wiley-VCH, 2008

/7/ Wolf, M.:
Minimierung des Druckverlusts durch Optimierung der CO-Entfernungsstufe für ein stationäres PEM-Brennstoffzellenheizgerät
Ph.D. thesis, Karlsruhe Institute of Technology (KIT), 2010

/8/ Moe, J. M.:
Design of water-gas shift reactors
Chem. Eng. Prog., 58 (1962), 33-36

/9/ Schulz, A.:
Selektive Methanisierung von CO in Anwesenheit von CO2 zur Reinigung von Wasserstoff unter den Bedingungen einer PEM-Brennstoffzelle
Ph.D. thesis, Universität Karlsruhe (TH), 2005

LIST OF TABLES

LIST OF FIGURES